Webster, R., Cherns, D., Kuball, M., Jiang, Q., & Allsop, D. (2015). Electron microscopy of gallium nitride growth on polycrystalline diamond. Semiconductor Science and Technology, 30(11), 114007. DOI: 10.1088/0268-1242/30/11/114007

Electron microscopy of gallium nitride growth on polycrystalline diamond

2015 Semicond. Sci. Technol. 30 114007

(http://iopscience.iop.org/0268-1242/30/11/114007)

OPEN ACCESS
IOP Publishing
Semiconductor Science and Technology
Semicond. Sci. Technol. **30** (2015) 114007 (6pp)
doi:10.1088/0268-1242/30/11/114007

Electron microscopy of gallium nitride growth on polycrystalline diamond

R F Webster[1], D Cherns[1], M Kuball[1], Q Jiang[2] and D Allsopp[2]

[1] H H Wills Physics Laboratory, University of Bristol, Tyndall Avenue, Bristol BS8 1TL, UK
[2] Department of Electrical and Electronic Engineering, University of Bath, Bath BA2 7AY, UK

E-mail: richard.webster@bristol.ac.uk

Received 28 March 2015, revised 3 August 2015
Accepted for publication 7 August 2015
Published 15 October 2015

Abstract

Transmission and scanning electron microscopy were used to examine the growth of gallium nitride (GaN) on polycrystalline diamond substrates grown by metalorganic vapour phase epitaxy with a low-temperature aluminium nitride (AlN) nucleation layer. Growth on unmasked substrates was in the (0001) orientation with threading dislocation densities $\approx 7 \times 10^9\,\mathrm{cm}^{-2}$. An epitaxial layer overgrowth technique was used to reduce the dislocation densities further, by depositing silicon nitride stripes on the surface and etching the unmasked regions down to the diamond substrate. A re-growth was then performed on the exposed side walls of the original GaN growth, reducing the threading dislocation density in the overgrown regions by two orders of magnitude. The resulting microstructures and the mechanisms of dislocation reduction are discussed.

Keywords: gallium nitride, growth, electron microscopy, polycrystalline diamond

(Some figures may appear in colour only in the online journal)

Introduction

Diamond is an attractive material for electronic applications as it has one of the highest known thermal conductivities at $\approx 2000\,\mathrm{Wm}^{-1}\,\mathrm{K}^{-1}$ [1]. Using diamond as a substrate for high electron mobility transistors (HEMTs), or light emitting diodes could improve the performance and lifetime of such devices by allowing them to operate at lower temperatures than they would on conventional substrates such as sapphire, silicon or silicon carbide (SiC) [2]. Single crystal diamond however is expensive so is not currently a realistic substrate to grow on commercially. Polycrystalline diamond is grown on silicon by chemical vapour deposition (CVD) methods [3] however retains a high thermal conductivity, albeit less than single crystal diamond [4, 5], whilst also being more affordable.

Growth of GaN on crystalline diamond and polycrystalline diamond is inherently difficult however as there is a large lattice mismatch between the two materials around 13% which will likely generate mismatch defects and lead to poor crystal quality [6–8]. Other issues are the large difference in coefficient of thermal expansion between the two materials ($4.38 \times 10^{-6}\,\mathrm{K}^{-1}$ and $5.59 \times 10^{-6}\,\mathrm{K}^{-1}$ for diamond and GaN respectively [8]) which could lead to cracking of the GaN layer, and the absence of a fixed epitaxial relationship between the GaN and a polycrystalline diamond substrate making the nucleation of continuous epitaxial GaN layers problematic. The lack of epitaxy and lattice mismatch may be partially overcome by using a low-temperature AlN buffer layer between the GaN and the substrate, a technique used in the growth of GaN on conventional substrates such as Si and SiC [9]. This generates island growth of AlN preferentially in the [0001] direction directly on the substrate reducing the lattice mismatch and enhancing GaN nucleation on the substrate.

Another potential solution would be to grow GaN conventionally on a 'dummy substrate' of silicon or sapphire, then remove the substrate and bond the GaN to diamond. This however has the disadvantage of introducing a thermal blocking layer (the bonding material) between the GaN and the diamond which could hinder the lattice vibrational

phonons which transfer the heat negating the effect of the high thermal conductive substrate.

Experimental

GaN epitaxial layers were grown on polycrystalline diamond in an AIX200/4HT-S metalorganic vapour phase epitaxy (MOVPE) system with a low temperature AlN as a nucleation layer. Before growth the substrate temperature was raised to approximately 1000 °C for 10 min to conduct a thermal cleaning process, the substrate temperature was then decreased to ≈650 °C to form an Al monolayer. An AlN nucleation layer was deposited at a pressure of 100 mbar and NH3, Trimethylaluminium (TMAl) and H2 carrying gas flow rates of ≈1200 standard litres per minute (SLM), ≈23 SLM and ≈4.5 SLM respectively. Finally, a 1.5 μm GaN layer, an AlN space layer (≈2 nm) and a 20 nm AlGaN barrier layer were deposited at 1060 °C.

In order to provide a GaN buffer layer of high-quality for devices, the above nucleation process was combined with epitaxial layer overgrowth (ELOG) growth to reduce the density of threading defects in the epitaxial III-nitride heterostructure. A GaN/AlN/PD template was patterned into GaN (10-10) stripes with inductively coupled plasma etching and a Ni layer (∼200 nm) as an etching mask. Afterwards, a growth mask (Si_xN or SiO_2) was carefully fabricated onto the structure to allow the side-walls of the stripes exposed for an overgrowth to re-grow.

Transmission electron microscopy (TEM) samples were prepared using an FEI Helios dual beam focused ion beam (FIB) allowing scanning electron microscopy (SEM) to be taken simultaneously. First a 2 μm platinum layer was deposited to protect the surface layer from the gallium beam. Rough milling was performed with a gallium accelerating voltage of 30 kV until a thickness of approximately 100 nm was achieved then a low energy polish was performed at 5 kV. Prepared samples were then studied in a Philips EM430 TEM operated at 200 kV and on a JEOL 2010 operated at 160 kV.

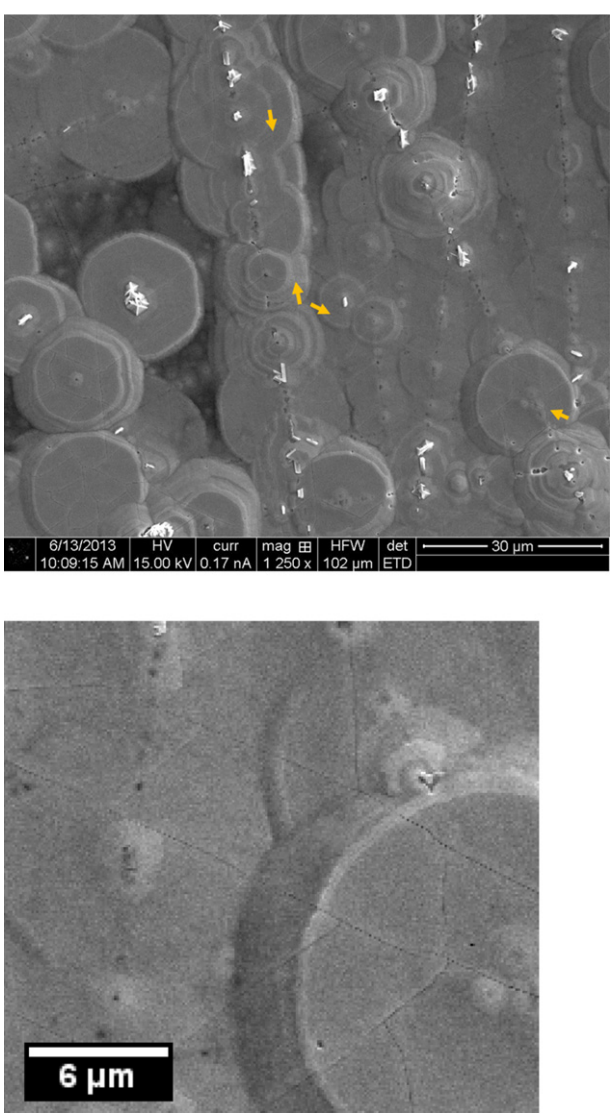

Figure 1. SEM of two samples (a) The GaN HEMT grown on polycrystalline diamond with arrows showing two examples of cracking and (b) an enlarged area of (a) showing the crack structure.

Results and interpretation

Figure 1(a) shows an SEM image of the surface of the unmasked sample where hillocks can be seen. These hillocks are 15 μm wide and form along lines which are associated with non-planar defects in the surface of the polycrystalline diamond substrate associated with its manufacture by plasma-assisted CVD on a silicon substrate. The SEM image shows sparse nucleation of hillocks which are well separated and have large amount of lateral growth. Some hillocks form rounded hexagons indicating GaN growth on the (0001) basal plane with sidewalls of the (10-1x) type. In the centre of most hillocks are pits, whereas in others there are some pits and additional structures, this could be associated with defects in the GaN and with final AlGaN growth. There is also some cracking in the GaN growth, highlighted in figures 1(a) and (b) by arrows, this is quite extensive and is continuous across multiple hillocks. The angle between such cracks is consistently 60° and the direction is along the same orientation as the sidewalls of the hillocks suggesting cracking is occurring along the (10-10) planes.

TEM images of this sample are shown in figure 2: this section is taken from the centre of a hillock outwards in the [10-10] direction such that the sample is viewed in the [11-20] direction. Towards the left of the figure the GaN is seen to slope downwards; this is the edge of the hillock. All layers of the sample can be seen on this figure: the polycrystalline diamond with a grain size of 1–2 μm at the bottom of the image. The AlN nucleation layer is 70 nm thick. The GaN grows to a height of 1.5 μm and has a high density of dislocations measured at 7×10^9 cm^{-2}. From the bottom to the top of the film there is a reduction in the number of dislocations by a factor of ≈3.

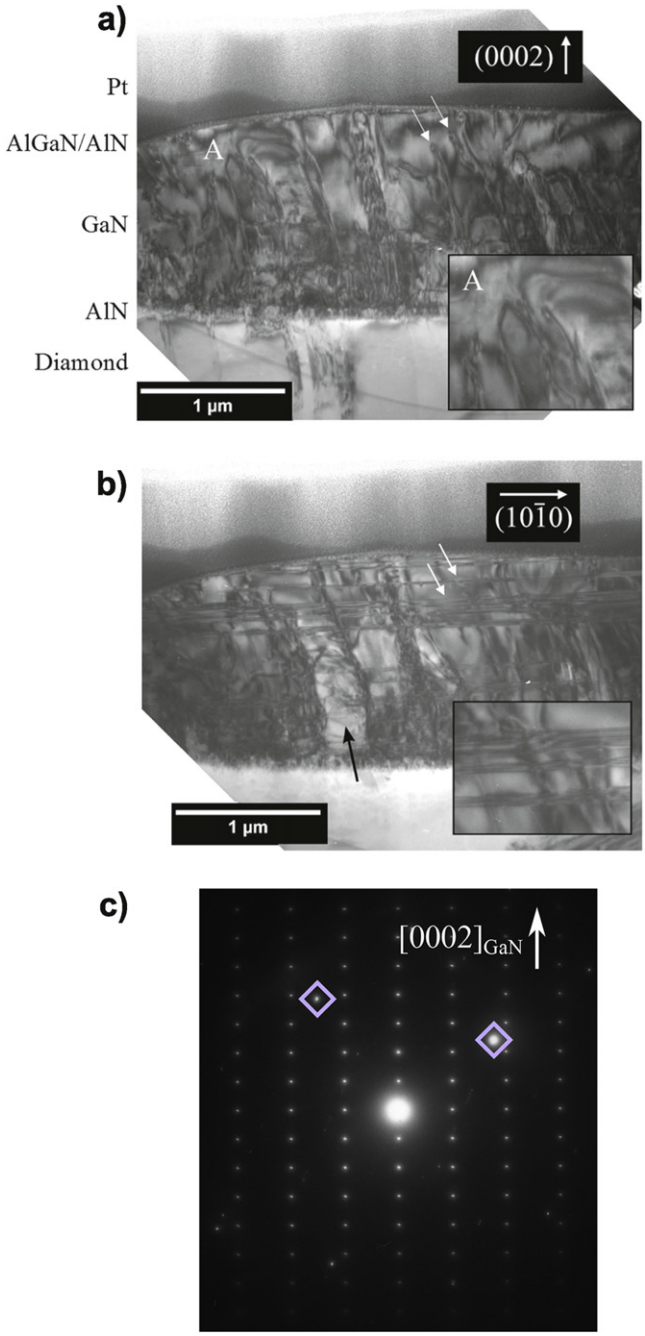

Figure 2. Two bright field TEM images of the GaN on PD sample in (a) **g** = (0002) and (b) **g** = (10-10) two-beam conditions. Two white arrows indicate the positions where threading dislocations (in the **g** = (0002) conditions) terminate at stacking faults. The inset of (a), taken from region 'A', shows the annihilation of two dislocations and the interaction of threading dislocations with stacking faults. A selected area electron diffraction pattern taken from a region including the GaN/diamond interface is shown in (c). This shows a [11-20] zone axis diffraction pattern of the GaN and two additional spots from the diamond substrate (highlighted in blue).

A selected area diffraction pattern taken over the GaN AlN/diamond interface is shown in figure 2(c). This shows the GaN oriented on the [11-20] zone axis. Additional diffraction spots from the diamond substrate (highlighted by blue squares) indicate no obvious orientation relationship between the GaN and the substrate in this area. However, the SEM images in figure 1 suggest that, on a longer range, there is a preferred orientation of the GaN which is likely to be related to a preferred orientation in the polycrystalline diamond film.

The image in figure 2(b) was taken in the **g** = (10-10) two beam condition where stacking faults and a-type and a + c type threading dislocations are visible [10]: stacking faults are seen to extend across the whole of the structure. The black arrow in figure 2(b) indicates a region of GaN which has brighter contrast to the surrounding GaN. This is caused by a slight misorientation which affects the diffraction conditions of this region. However, the stacking faults have been observed to continue through this region of the GaN. In contrast, in figure 2(a) in **g** = (0002) two beam conditions where c-type and a + c type dislocations are visible, the stacking faults are not seen and only residual contrast remains. However c-type threading dislocations are seen to bend over and terminate in stacking faults (arrowed in the figure). Tilting the sample has revealed that these dislocations do not move relative to the stacking fault implying that these are coincident. Other dislocations are observed to annihilate with each other. This is shown in the inset of figure 2(a). Some residual contrast is observed in the inset of the figure 2(b) (in **g** = (10-10) two beam conditions) from the same area as figure 2(a). This indicates that these may be a + c type dislocations, though this is obscured somewhat by the stacking faults visible in these imaging conditions.

These mechanisms are seen to reduce the dislocation density towards the top of the film. Furthermore, dislocations are seen to consistently tilt towards the top left of figure 2 which we interpret as an indication that there is significant lateral growth in the film.

The TEM image in figure 3 shows stacking faults nucleating within the GaN (in figure 3(b) in **g** = (10-10) two beam conditions) and comparison with **g** = (0002) images show (figure 3(a)) that these are not always associated with threading dislocations. Also in figure 3 there is a region of where the AlN buffer layer did not grow and the GaN has grown up and around this region forming a void. This suggests that the GaN is preferentially growing on the AlN rather than the diamond. Stacking faults are seen in the region over this void which extend across and only c-type treading dislocations are seen in the **g** = (0002) image.

Convergent beam electron diffraction (CBED) was performed with the sample orientated to the (0002) systematic row which reduces double diffraction into the (0002) disks resulting in a less ambiguous diffraction pattern. This is shown in figure 4 alongside a simulation performed in JEMS [11]. This shows that the film has grown with N-polarity, this could be due to the initial AlN being deposited as N-polar and this polarity is retained in the growth of GaN. CBED was performed across the sample with only a small variation in orientation which could be due to sample bending and no inversion of polarity was observed.

Figure 5 shows an SEM image of the ELOG growth, this growth has not met in the middle allowing the early stages of

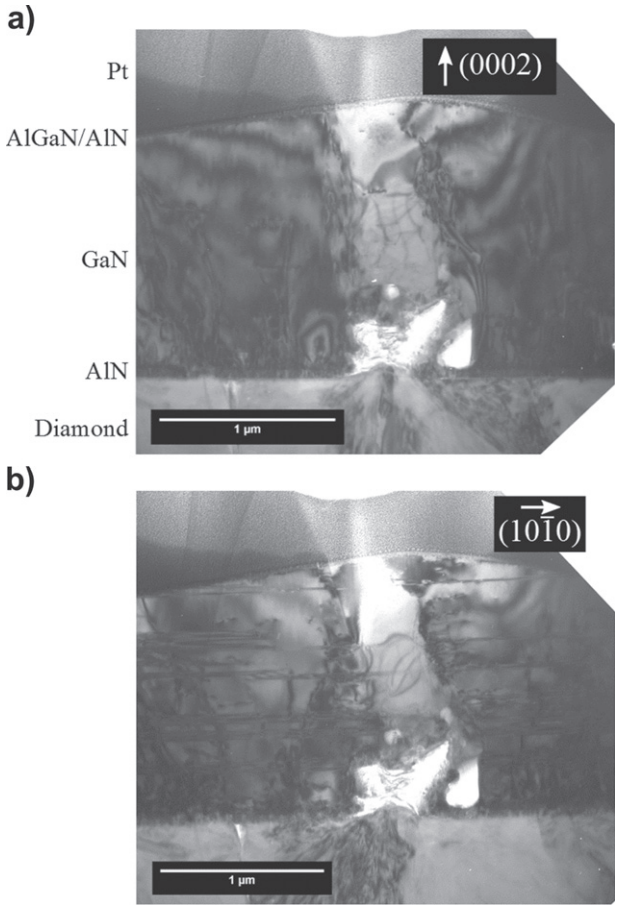

Figure 3. TEM image (a) in **g** = (0002) and (b) in **g** = (10-10) two-beam conditions showing the nucleation of stacking faults in the GaN.

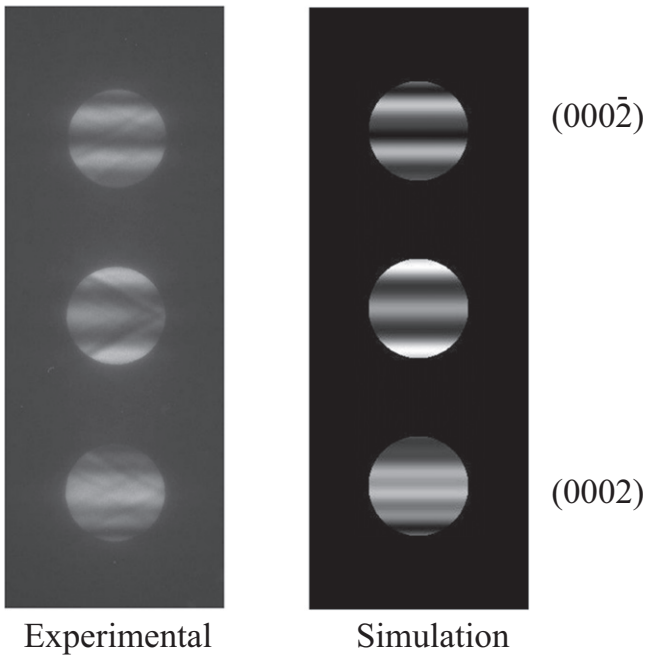

Figure 4. Experimental and JEMS simulated CBED patterns taken in the GaN film. In the experimental pattern the growth direction of the GaN film is towards the top of the page.

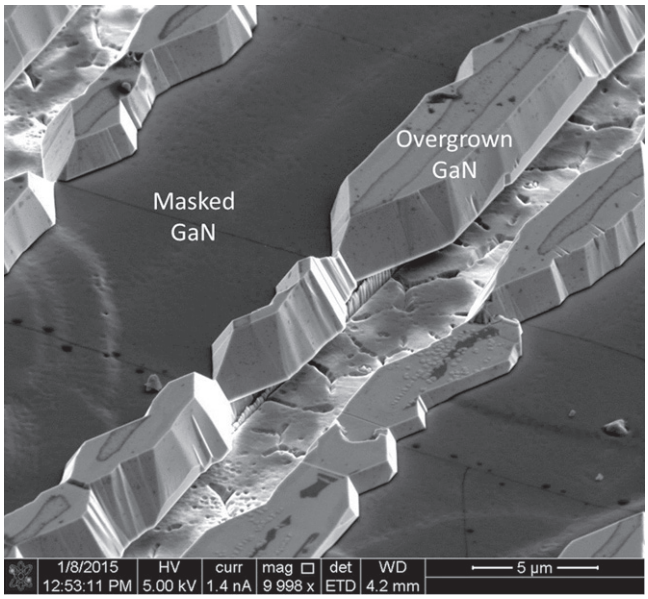

Figure 5. Labelled SEM image of the masked growth.

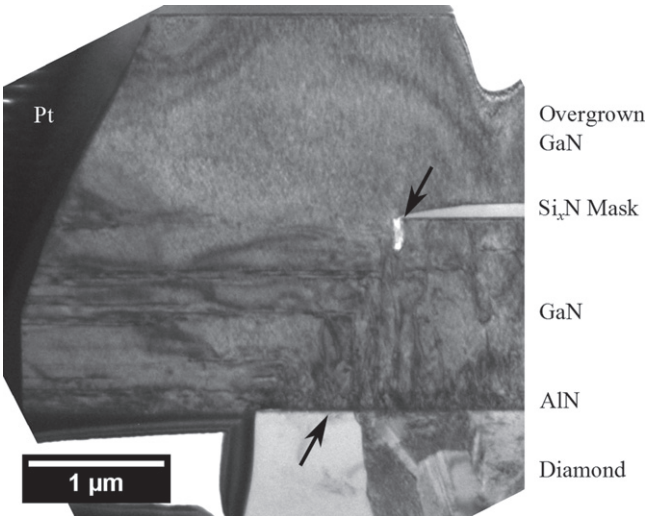

Figure 6. TEM of the ELOG region showing the original GaN growth with ELOG growth on the side walls growing around the mask. Arrows indicate the boundary between the original growth (right of the boundary) and the ELOG growth (left of the boundary).

growth to be observed. The masked GaN stripes are visible and these are similar to those in figure 1(a) with some evidence of hillocks on the surface. In the etched regions the substrate can be seen and the overgrown GaN can be seen growing laterally over this region as well as vertically.

Figure 6 shows a TEM image taken in the **g** = (10-10) two beam condition so the stacking faults, a-type and mixed dislocations are visible. This figure shows one side of the overgrowth, the diamond (with boundaries highlighted for clarity), the mask GaN, the etched region and overgrowth are visible. Surrounding the structure is the Pt deposit and there is some speckling in the overgrowth region which are both from the FIB sample preparation.

Moving right to left across figure 6, at the base is the original GaN growth which has a high density of dislocations,

at the point where the mask ends this is where the ELOG growth starts. The GaN is seen to grow laterally and overgrow the pits of the template. In this region the dislocations are seen to turn through 90° and continue until the left edge of the sample as threading dislocations on the basal plane. Where the growth is predominantly lateral there was a threading dislocation density lower than $10^8\,\mathrm{cm}^{-2}$.

The vertical growth is seen to be free of stacking faults and threading dislocations, this is also confirmed in $\mathbf{g} = (0002)$ two beam conditions (not shown). The second growth is seen to grow over the top of the mask and is 1 μm taller than the original GaN growth suggesting there is significant vertical growth.

Discussion

Our observations show the ability to grow GaN up to 15 μm wide with a significant degree of epitaxial orientation on a polycrystalline diamond substrate, which is encouraging for potential devices. The SEM of figure 1 also suggests that there some common orientation between the islands and the misorientation around the *c*-axis of the GaN is measured from the SEM (figure 1(a)) to be ±3° between hillocks. Cracks on the surface of the GaN were observed in SEM and these are probably due to the large thermal expansion difference between diamond and GaN which results in the GaN being in tension. These cracks can be followed across separate hillocks and are orientated at 60° to each other which strongly suggests that the cracks are along crystallographic planes. This is surprising as it would be expected that the growth on a polycrystalline substrate where the grain size is 1–2 μm (as the diamond is here) would result in larger misorientations than those seen. That is to say, nucleation of GaN on separate diamond grains would not necessarily produce growth in the [0001] direction. Yet we observe widespread growth in the [0001] direction which, is good for the reduction of defects and therefore thermal transport. The reason for this is likely to be the AlN nucleation layer which even on amorphous SiO_2 can produce [0001] GaN [12]. This point is emphasized by the selected area diffraction pattern (in figure 2(c)) where the GaN grows in the [0001] direction though the adjacent diamond is not orientated in this direction.

It was also observed in SEM (figure 1(a)) and TEM (figure 2) of the unmasked sample that there was up to five times more lateral growth than vertical growth. It seems that the GaN is nucleating at well separated points on the substrate (more than 30 μm apart in some cases) with some preference to nucleate along scratches on the diamond substrate. These once nucleated rapidly grow laterally to generate these wide islands. We can say this with some certainty as (a) electron diffraction showed the orientation of the GaN in the TEM sample varied by only a small amount from the [11-20] direction across the sample and was likely due to bending of the sample rather than sub-grains, and (b) the stacking faults form in the centre of the GaN (figure 3) and extend laterally to the surface of the GaN a distance of up to 8 μm, implying these are of one continuous lateral growth. Furthermore, threading dislocations are tilted to the left which suggests direction of the growth is tilted from the [0002] direction. From these observations we infer that the growth is taking place on steps on the (0001) planes which facilitates the lateral growth, enabling the stacking faults to grow to such lengths. That is to say, once a stacking fault forms (either because of a fault in the stacking sequence or the dissociation of a threading dislocation) the large lateral growth rate means that it quickly expands to cover a large area. This process is likely to be facilitated by the lateral migration of surface steps. Furthermore, the interaction of these surface steps with the threading dislocations in the GaN causes the threading dislocations to become inclined.

The CBED patterns of figure 4 showed that the GaN is N-polar. This is likely to be determined by the polarity of the AlN buffer layer and suggests that Al-C bonds are forming initially at the interface of the AlN and the diamond which would give the AlN N-polarity. However, this needs further investigation to be confirmed.

Figure 6 shows that the ELOG sample shows promise and that it may be possible to achieve high quality GaN on polycrystalline substrates. Dislocations would be expected at the points where the wings meet as has been seen in previous ELOG growths. The threading dislocations from the original growth are observed to bend over and terminate at the edges of the lateral growth, this is likely due to the relief of tensile stress at the lateral surface of the GaN [13]. However, the overall dislocation density is expected to reduce significantly using this technique, as is seen in the GaN which has grown above the masked area where no threading dislocations are observed.

Conclusion

We have grown and studied by TEM two GaN samples grown on polycrystalline diamond one as-grown and the second with an ELOG technique applied. In the as-grown sample the surface was rough with the GaN forming hillocks 15 μm wide and a misorientation of up to 6° between these hillocks. Despite the growth being on polycrystalline diamond, this paper has demonstrated that it is possible to grow high quality, low defect density GaN without necessarily requiring masking to promote lateral growth. This is owing to the low density of GaN islands and subsequent promotion of extensive lateral growth which reduces defect density by lateral migration and annihilation of dislocations. When the ELOG technique is applied the dislocation density is reduced further due to a predominant lateral growth in the [10-10] direction with dislocations turning over and terminating at surfaces. This results in a dislocation free growth above the masked area.

Acknowledgments

Authors would like to thank Dr I Griffiths of the University of Bristol for his assistance with FIB sample preparation. This

work was funded by the Engineering and Physical Sciences Research Council (EPSRC) under grants EP/K024345/1 and EP/K024337/1.

References

[1] May P 2000 Diamond thin films: a 21st-century material *Phil. Trans. R. Soc.* A **358** 473–95
[2] Felbinger J and Chandra M 2007 Comparison of GaN HEMTs on diamond and SiC substrates *Device Lett. IEEE* **28** 948–50
[3] Ashfold M N R, May P W, Rego C A and Everitt N M 1997 Thin film diamond by chemical vapour deposition methods *Chem. Soc. Rev.* **23** 21–30
[4] Yamamoto Y, Imai T, Tanabe K, Tsuno T, Kumazawa Y and Fujimori N 1997 The measurement of thermal properties of diamond *Diam. Relat. Mater.* **6** 1057–61
[5] Hartmann J, Voigt P and Reichling M 1997 Measuring local thermal conductivity in polycrystalline diamond with a high resolution photothermal microscope *J. Appl. Phys.* **81** 2966–72
[6] Dussaigne A, Malinverni M, Martin D, Castiglia A and Grandjean N 2009 GaN grown on (111) single crystal diamond substrate by molecular beam epitaxy *J. Cryst. Growth* **311** 4539–42
[7] Alomari M, Dussaigne A, Martin D, Grandjean N, Gaquière C and Kohn E 2010 AlGaN/GaN HEMT on (111) single crystalline diamond *Electron. Lett.* **46** 299
[8] Hageman P R, Schermer J J and Larsen P K 2003 GaN growth on single-crystal diamond substrates by metalorganic chemical vapour deposition and hydride vapour deposition *Thin Solid Films* **443** 9–13
[9] Hageman P R, Haffouz S, Kirilyuk V, Grzegorczyk A and Larsen P K 2001 High quality GaN layers on Si (111) substrates: AlN buffer layer optimisation and insertion of a SiN intermediate layer *Phys. Status Solidi* A **188** 523–6
[10] Ponce F A, Cherns D, Young W T and Steeds J W 1996 Characterization of dislocations in GaN by transmission electron diffraction and microscopy techniques *Appl. Phys. Lett.* **69** 770
[11] Stadelmann P A 1987 EMS a software package for electron diffraction analysis and HREM image simulation in materials science *Ultramicroscopy* **21** 131–45
[12] Leung B, Song J, Zhang Y and Han J 2013 Evolutionary selection growth: towards template-insensitive preparation of single-crystal layers *Adv. Mater.* **25** 1285
[13] Liliental-Weber Z and Cherns D 2001 Microstructure of laterally overgrown GaN layers *J. Appl. Phys.* **89** 7833